

# Computational Screening of Weak Hydrogen Bond Networks: Predicting Stable Structures for Difluoromethane Oligomers

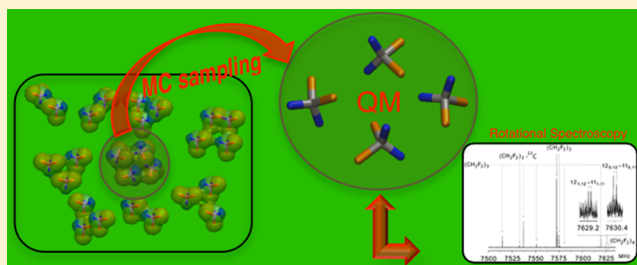
Giacomo Prampolini,<sup>†</sup> Laura Carbonaro,<sup>‡</sup> Gang Feng,<sup>§</sup> Luca Evangelisti,<sup>§</sup> Walther Caminati,<sup>§</sup> and Ivo Cacelli<sup>\*,‡</sup>

<sup>†</sup>Istituto di Chimica dei Composti OrganoMetallici (ICCOM-CNR), Area della Ricerca, via G. Moruzzi 1, I-56124 Pisa, Italy

<sup>‡</sup>Dipartimento di Chimica e Chimica Industriale, Università di Pisa, Via Risorgimento 35, I-56126 Pisa, Italy

<sup>§</sup>Dipartimento di Chimica "G. Ciamician", Università di Bologna, Via Selmi 2, I-40126 Bologna, Italy

**ABSTRACT:** The stability and the structure of small difluoromethane oligomers are studied by combining classical Monte Carlo and quantum mechanical calculations. A hierarchical procedure was adopted to validate the accuracy of the whole protocol: the force field used in Monte Carlo simulations is parametrized on the basis of dimer intermolecular energies computed with density functional theory. The density functional is similarly chosen by comparing the interaction energies with reference values, purposely computed at a coupled cluster level, extrapolated at the complete basis set. The structures of dimers, trimers, and tetramers identified by the screening as local minima are first characterized by some geometrical parameters and by their dipole moment and eventually validated by comparison with results of microwave spectroscopy. The results are found in very good agreement with the experiment for all considered structures.



## INTRODUCTION

The impressive growth of the field of fluoroorganic chemistry<sup>1–4</sup> in recent years is certainly due to its impact on biomedical chemistry and materials science. Indeed, many advanced materials such as polymers or liquid crystals owe their unique properties to the influence of fluorinated structures.<sup>1,5</sup> Moreover, many modern pharmaceuticals contain one or more fluorine atoms that often serve very specific functions.<sup>3</sup> Yet, fluoroorganic compounds, and in particular fluorocarbons, are stimulating also from a more fundamental point of view. Their physical properties can be connected to the extremely low polarizability of fluorine, which in turn derives from the combination of high electronegativity with moderate size. In perfluoroalkanes, the carbon–fluorine dipole moments cancel each other for symmetry reasons, making their intermolecular interactions rather weak. Conversely, quite strong electrostatic interactions are observed when hydrocarbons are only partially fluorinated, in particular if the bonds to fluorine and hydrogen arise from the same carbon atom.<sup>4</sup> In this case, due to polarization of the C–H bonds, the aliphatic hydrogen atoms acquire acidic character and the fluorine atom can act as an acceptor.

The simplest example reported<sup>6</sup> for this effect is difluoromethane CH<sub>2</sub>F<sub>2</sub> (DFM). In their work, Caminati et al. employed rotational resolved spectroscopy, flanked by theoretical calculations, to assess whether DFM can form a hydrogen-bonded dimer similarly to the water molecule, acting as a double proton donor and as a double proton acceptor.<sup>6</sup> Indeed, the most stable DFM dimer was characterized by a network of three weak hydrogen bonds (WHB), established

between the neighboring C–H/C–F pairs. As far as DFM oligomers are concerned, trimers<sup>7</sup> were also investigated by both rotational spectroscopy and quantum mechanical (QM) calculations. A number of weak unassigned bands of the molecular beam rotational spectrum was found<sup>7</sup> consistent with the structure of a stable trimer determined by a theoretical approach. More recently,<sup>8</sup> the rotational spectrum of DFM tetramers has also been reported, together with the structures rationalized by QM calculations. In both of these works, the comparison of QM calculations with rotationally resolved spectroscopy has been proven capable of yielding precise information on dimers and larger oligomers, supplying data that allow for a deeper understanding of the chemical features of multiple WHB networks.

In this context, the possibility of setting up an a priori screening procedure to spot the most probable conformers of small molecular clusters, thus addressing the experimental search, is certainly appealing. Such an approach integrates the accuracy of QM calculations with the effectiveness of classical sampling methods.<sup>9</sup> From a computational point of view, the main problem lies in the presence of the large number of quasi-degenerate structures that can be expected as outcome from the automated screening since one has to deal with many local minima in the domain of both intramolecular and intermolecular coordinates, often connected by small energy gaps. In this scenario, reliable calculations require exploring a very large number of conformations<sup>9</sup> in order to minimize the possibility

Received: February 20, 2014

Published: April 14, 2014



of neglecting important structures. Post-HF level of theory, which is often used for single point calculations, is therefore not suitable for works of this type. Rather, one can resort to cheaper calculations based on density functional theory (DFT), which is used more and more for the evaluation of intermolecular energies and geometries.<sup>10–19</sup> Although for DFM systems we can expect that electrostatic forces play a very relevant role in the energetics of the oligomers, the dispersion terms should not be neglected in order to get reliable results. A popular way to take into account dispersion forces within DFT is the DFT-D method,<sup>11,15,19,20</sup> in which the dispersion energy is added to the standard DFT energy, through empirical atom–atom terms. In view of the large number of proposals which can be found in the literature,<sup>11,13–15</sup> the choice of the functional and dispersion terms can be driven by high level calculations of few selected geometries of the DFM dimer. As a high-level reference method, in this work the coupled-cluster extrapolated at complete basis set (CCSD(T)@cbs) protocol was chosen, which was separately proposed in slightly different implementations by the groups of Tsuzuki,<sup>21</sup> Hobza,<sup>10,22</sup> and Sherrill,<sup>16,23</sup> and often referred to<sup>24</sup> as the “gold standard” of quantum chemistry, concerning the intermolecular interactions.

Finally, from a more fundamental point of view, another aspect will be investigated in the present study. As reported in ref 6, the DFM dimer presents a blue shift in the C–H stretching frequencies and a shortening of the C–H bond lengths, with respect to the DFM monomer. As a matter of fact, these features were first reported both in computational<sup>25</sup> and experimental<sup>26</sup> studies, performed on the benzene dimer and on a dimer fluoro-benzene/chloroform complex, respectively. It may be worth mentioning that in these early papers, the weak hydrogen bond (WHB) between H and F atoms was labeled as “anti-H bond”, in consideration of the blue shift registered in the vibrational frequency and in contrast with the red shift usually found for a proper hydrogen bond (HB). Soon after, this definition was found misleading, and the terms “improper” or blue-shifted HBs were proposed<sup>27</sup> instead. In the past decade, the presence of improper HBs in the context of WHBs has been investigated and confirmed in several dimer compounds, both theoretically<sup>27–31</sup> and experimentally,<sup>6,32–36</sup> proving its importance in recognition and binding in chemical and biological systems. Recently,<sup>29</sup> a unified explanation of the vibrational features of the WHBs has been given in terms of electron affinity of the atom bearing the hydrogen and intensity of the H-acceptor interaction. However, to our knowledge, no investigations have been reported in the literature on the behavior of WHBs in large oligomers.

This article is organized as follows: after a detailed description of the proposed screening protocol, the efficiency of the approach is tested by finding and characterizing the most stable structures of increasingly larger DFM oligomers. Eventually, a final validation of the computational procedure will be obtained by comparing the results with some experimental counterparts, obtained by rotational spectroscopy. Finally, the presence of WHB specific vibrational features (such as blue shift and bond shortening) will be discussed for DFM dimers, trimers, and tetramers.

## SCREENING PROTOCOL

The screening protocol was set up as sketched in the flowchart reported in Figure 1. First, the approach has to be tuned on the target molecular species. This is done in three steps:

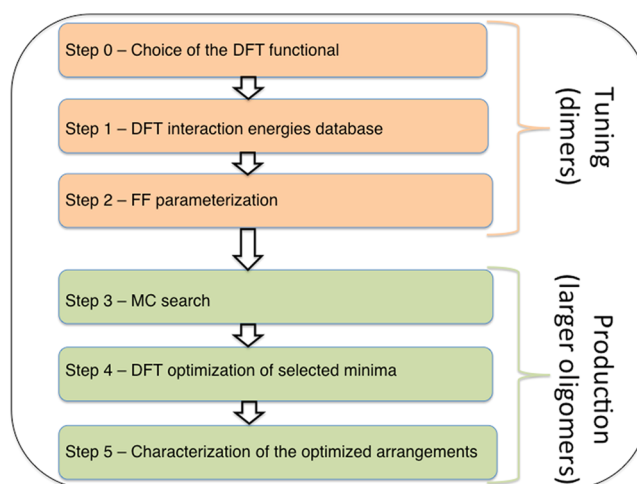


**Figure 1.** Scheme of the screening protocol adopted for DFM oligomers.

(0) Few reference dimer arrangements (obtained by preliminary optimizations and/or from literature data) are selected, and their interaction energy is computed at CCSD(T)@c.b.s level of theory. The resulting data are then used as the target to benchmark several DFT functionals, eventually choosing the one which better agrees with reference CCSD(T)@c.b.s data.

(1) The chosen functional is used to sample the dimer potential energy surface with a large number of arrangements to be used for the next step.

(2) The parameters of an intermolecular force field (FF), composed of Coulomb and Lennard-Jones functions, are optimized by a least-squares fitting procedure using as reference the DFT computed dimer energies. The method was already described in previous papers.<sup>37,38</sup>

Once the FF is obtained, the search and the characterization of stable dimers as well as trimers and tetramers can be performed. Despite the fact that chemical intuition can help to spot some of the most stable oligomer arrangements, a more systematic approach was adopted. This “production” phase can be summarized also in three steps:

(3) A Monte Carlo (MC) method, using the FF determined in step 2, was run, and all the structures corresponding to local minima were stored.

(4) The stored MC geometries were used as the starting point of geometrical DFT optimizations. As expected, many of them converge to the same geometrical arrangements, but a number of different structures can be obtained.

(5) These latter structures were finally characterized by computing the rotational constants and the vibrational frequencies.

## COMPUTATIONAL DETAILS

Reference data were obtained at the CCSD(T) level of theory estimated at the complete basis set limit, obtained by exploiting the following empirical approximate relationship:

$$\Delta E_{\text{cbs}}^{\text{CCSD(T)}} - \Delta E_{\text{TZ}}^{\text{CCSD(T)}} = \Delta E_{\text{cbs}}^{\text{MP2}} - \Delta E_{\text{TZ}}^{\text{MP2}}$$

where  $\Delta E$  is the binding energy of the dimer and the subscripts TZ and cbs indicate the triple- $\zeta$  basis set aug-cc-pVTZ and the complete basis set, respectively. The value of  $\Delta E_{\text{cbs}}^{\text{MP2}}$  was estimated by the extrapolation formula of Halkier et al.<sup>39</sup> from

the aug-cc-pVTZ and aug-cc-pVQZ results. As detailed in the following, we found that the B97D functional of Grimme,<sup>20</sup> coupled with the aug-cc-pVTZ basis set, was accurate enough to furnish reliable results of both binding energies and geometries, at least for the considered DFM dimers. Therefore, all of the trimer and tetramer structures were computed at the B97D/au-cc-pVTZ level of theory.

The MC program was written in our group to sample at a low computational cost a very large number of arrangements of oligomers. In this step, the temperature has to be tuned to rather low values, in order to explore a large number of possibilities without exceeding in exploring high-energy conformations. The trial MC moves included translations and rotations, whereas no internal moves were allowed. The lowest energy conformations of each oligomer were extracted from the MC run and stored in a database. In order to avoid storing very similar conformations, a resemblance test was put in the MC program. All quantum chemical calculations were performed using the Gaussian 09 package.<sup>40</sup>

## RESULTS AND DISCUSSION

The first step concerns the test of the density functional as compared with the high level calculation CCSD(T) extrapolated at the complete basis set. As the target sample, four selected dimer arrangements were prepared as detailed in the following: the **A1** dimer was obtained by a full geometry optimization, performed at the B97D/au-cc-pvDz level, starting from the dimer conformation indicated in ref 6; the **A2** dimer was built by rotating **A1** until only two H...F bonds are formed; **A3** was obtained from **A2** by a 60° rotation around the C...C vector; and **A4** was derived from **A3** by increasing the C...C to 3.2 Å. All arrangements are reported in Figure 2.

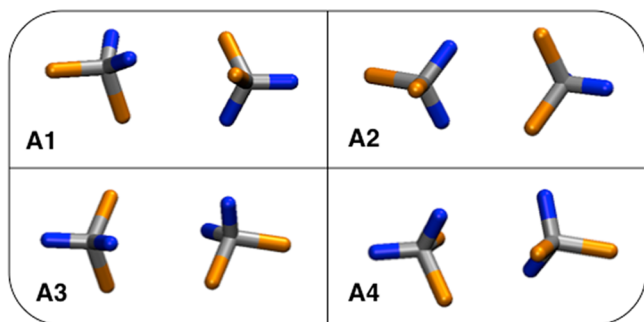


**Figure 2.** Selected DFM dimer arrangements employed in CCSD(T)@cbs benchmark calculations.

Binding energies were computed for each arrangement, both at the CCSD(T)@cbs and DFT level. In the latter case, the B97D functional proposed by Grimme<sup>20</sup> was employed and tested with different basis sets. Finally, binding energies were computed with and without the standard counterpoise correction<sup>41</sup> for the basis set superposition error (BSSE).

By looking at the results reported in Table 1, it is apparent that BSSE correction tends to worsen the agreement with the reference data, in accordance with the philosophy of Grimme<sup>20</sup> who parametrized the empirical dispersion parameters in such a way to include the BSSE correction. The results for the two basis sets without correction are not too different confirming the modest DFT dependence on the basis set as compared with post-HF calculations. The best result is, however, obtained with the aug-cc-pVTZ basis set, whose standard deviation is 0.14

**Table 1.** Comparison of B97D/au-cc-pvDz, B97D/au-cc-pvTz, and CCSD(T)@cbs Binding Energy (BE, kcal/mol) for the Four Selected DFM Geometries<sup>a</sup>

dimer	aug-cc-pVDZ		aug-cc-pVTZ		CCSD(T)@cbs
	unc	corr	unc	corr	
<b>A1</b>	−2.82	−2.36	−2.84	−2.64	−3.09
<b>A2</b>	−1.83	−1.57	−1.75	−1.62	−1.88
<b>A3</b>	−1.39	−0.85	−1.34	−0.16	−1.51
<b>A4</b>	−1.60	−1.33	−1.51	−1.42	−1.39
St. Dev.	0.18	0.27	0.14	0.52	

<sup>a</sup>Both BSSE uncorrected (unc) and corrected (corr) energies are reported for two basis sets employed with the B97D functional.

kcal/mol. These results can be considered accurate enough, also considering the intrinsic error in the extrapolation process that may be roughly estimated to be of the same order of magnitude. Therefore, unless otherwise stated, the B97D/au-cc-pVTZ level of theory is used all throughout the present work.

To complete the tuning phase (see Figure 1), steps 1 and 2 were performed. A number of significant geometries of the dimer are selected, and their B97D binding energies are used to parametrize a LJ+Q force field, to be used in MC calculations. The results are reported in Figure 3, together with a sketch of the considered dimer arrangements.

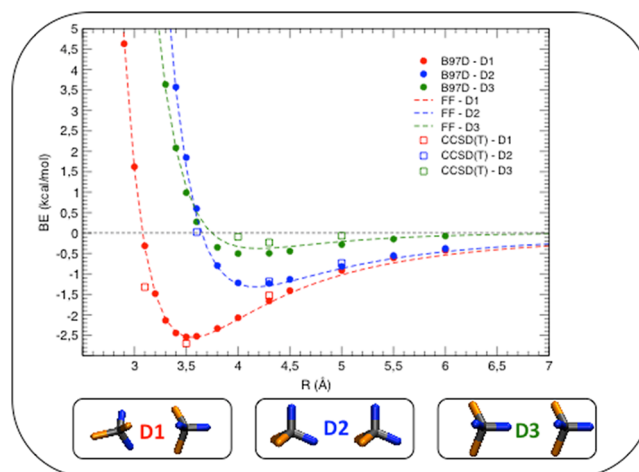


**Figure 3.** Comparison of CCSD(T), B97D, and FF binding energy (BE, kcal/mol) for three selected curves of the DFM dimer. *R* is the distance between the carbon atoms.

The FF energies are very close to the DFT ones above all for the most attractive curves with small discrepancies in the green curve corresponding to the unlikely relative position of two DFM molecules. For a more stringent validation, CCSD(T)@cbs binding energies were also computed for selected geometries along each curve (see Figure 3), and the parametrized FF also shows good agreement with the higher level calculations. These data make us confident that the present FF can be considered accurate enough to be confidently used in calculations that require a very fast evaluation of the dimer energy. In the hypothesis that three-body effects are negligible, this FF can be extended to the calculation of small oligomers studied in the present article.

Following the steps of the production phase (see Figure 1), the MC run can be now carried out for molecular clusters of

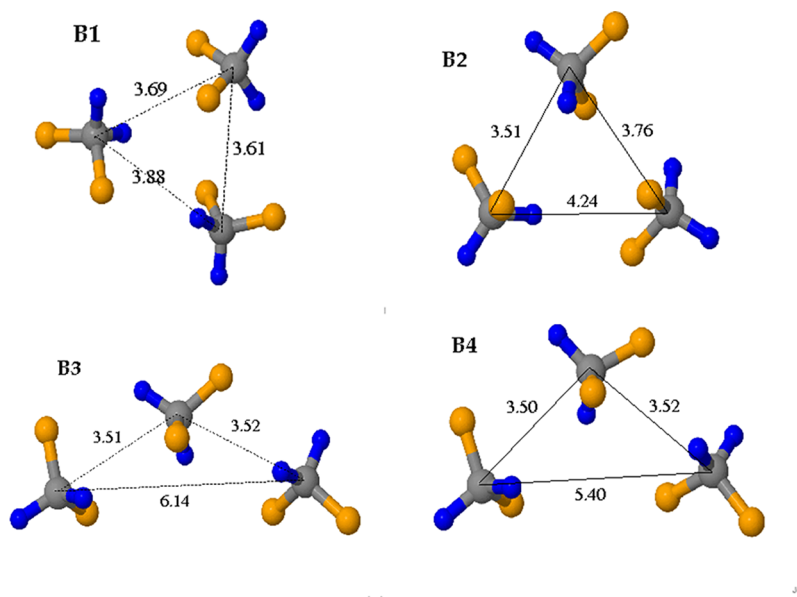


**Figure 4.** Geometrical structure of the four most stable DFM trimers. Distances are among carbon atoms (Å). The colors of the atoms are H = blue, fluorine = orange, and carbon = gray.

**Table 2.** Some Properties of the Four Most Stable Trimers of DFM Obtained by the Present Method<sup>a</sup>

trimer	BE	A	B	C	$\mu_A$	$\mu_B$	$\mu_C$	$\mu_{TOT}$	$N_{HF}$
B1	6.76	1322.5	804.6	592.8	2.14	0.63	0.44	2.28	014 020
B2	6.48	1150.1	954.5	645.3	0.59	1.17	0.71	1.49	032 001
B3	5.99	2234.6	461.5	418.8	2.17	0.04	0.78	2.31	004 021
B4	5.97	1688.9	590.0	484.6	1.68	0.39	0.76	1.88	013 012
exp <sup>7</sup>		1336.4	820.5	592.7	strong	weak	weak		
MP2 <sup>7</sup>		1380.1	843.1	611.2	2.4	0.6	0.6		

<sup>a</sup>BE is the binding energy (kcal/mol), A, B, and C are the rotational constants (MHz),  $\mu$  is the dipole moment (Debye) along the principal inertia axes, and  $N_{HF}$  is a composite number (see text) intended to summarize some geometrical features. The lowest two rows contain the experimental and calculated values, both from ref 7.

increasing size (i.e., dimers, trimers, and tetramers) in order to explore as much as possible the PES of the oligomer under study. The temperature must be adequately tuned in order to populate the most attractive regions of the multidimensional PES as well as to cross the energy barriers connecting two local energy minima. Test calculations indicate that the most adequate temperatures are in the 10–20 K range. A typical MC run includes more than  $10^6$  moves including translation and rotation of a random chosen monomer. In the starting configuration, the monomers were placed at large distances and rotated by different Euler angles. Because of the attractive potential, in the first part of the MC trajectories the monomers approach each other and give rise to stable oligomers. Owing to the relatively low energy barriers among the several local minima, many stable conformations are easily populated in the last part of the MC trajectory. Many different dimer, trimer, and tetramer conformations are then stored.

**Dimer.** The dimer was calculated in order to obtain data useful for the analysis of the higher oligomers. The conformation is very similar to that reported by Caminati et al.<sup>6</sup> The stability is mainly provided by three H...F intermolecular WHBs that, together with a smaller dispersion energy, accounts for a binding energy of 3.00 kcal/mol. Thus, a rough estimate of the stabilization energy provided by each H...F intermolecular interaction is  $\sim 1$  kcal/mol. According to Caminati et al.,<sup>6</sup> the internal geometry of the DFM in the dimer

is very similar to that of the isolated molecule. In fact, only a small shortening of the C–H distances was observed, again in agreement with ref 6.

**Trimer.** Each conformation stored in the MC run is used as the starting point of a B97D/aug-cc-pVTZ geometry optimization. The energy minimum of each optimized geometry was tested by computing the harmonic frequencies that were positive in all cases, indicating a positive definite Hessian. We employed about 20 conformations sorted from an MC run and obtained four distinct trimers, corresponding to the stable conformations shown in Figure 4. Each arrangement was characterized by computing binding energies, rotational constants, dipole moments, and stretching frequencies. Some of these properties are reported in Table 2.

A detailed analysis of the DFM trimer including a comparison between theoretical and experimental data was already reported elsewhere.<sup>7</sup> In that paper, the theoretical calculations were performed at MP2/6-311++G(d,p), and the results were accurate enough to allow the authors to elucidate the main features of the most stable trimer observed by rotational spectroscopy. Therefore, only a short discussion will be given here, mainly aimed to validate the present method through a comparison with the previous theoretical and experimental data.

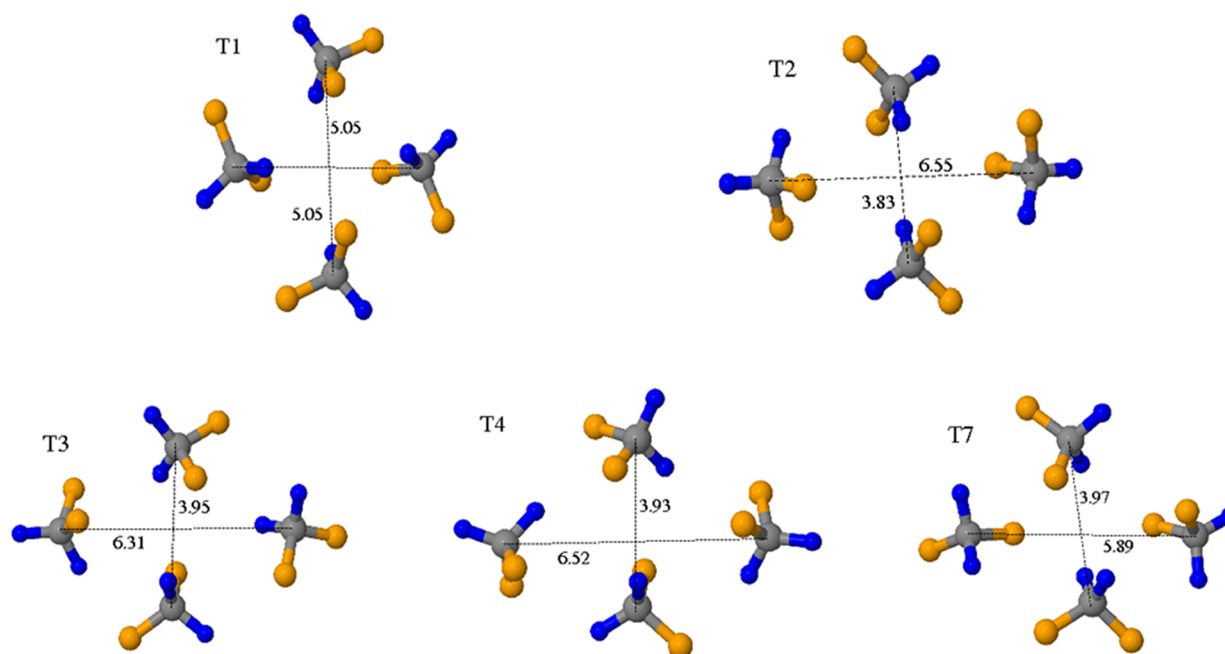
The agreement of the most stable trimer (B1) with experimental rotational constants is even better than that in



Table 3. Some Properties of the Seven Most Stable Tetramers of DFM<sup>a</sup>

tetramer	BE	A	B	C	$\mu_A$	$\mu_B$	$\mu_C$	$\mu_{TOT}$	LSP	$N_{HF}$
T1	11.52	620.1	619.9	357.2	0.00	0.00	0.00	0.00	0.067	044 000
T2	10.82	795.6	463.1	344.3	0.00	0.00	0.00	0.00	0.00	040 332
T3	10.79	835.9	403.6	313.1	2.85	0.12	0.47	2.89	0.31	034 140
T4	10.64	668.9	459.9	404.1	1.06	0.58	0.40	1.28	0.13	044 211
T5	10.50	823.1	433.3	335.5	1.92	0.93	0.65	2.23	1.24	135 110
T6	10.21	622.3	466.6	408.9	2.30	0.25	1.15	2.58	1.23	124 121
T7	10.14	684.7	454.9	344.9	3.21	2.21	0.23	3.90	0.61	134 030

<sup>a</sup>BE is the binding energy (kcal/mol); A, B, and C are the rotational constants (MHz);  $\mu$  is the dipole moment (Debye) along the principal inertia axes; LSP is the standard deviation (Å) of the least square plain of the four carbon atoms; and  $N_{HF}$  is the composite number also reported in Table 2.



**Figure 5.** Geometrical structure of the five DFM tetramers having near planar conformation. Distances are between carbon atoms (Å). The colors of the atoms are H = blue, fluorine = orange, and carbon = gray.

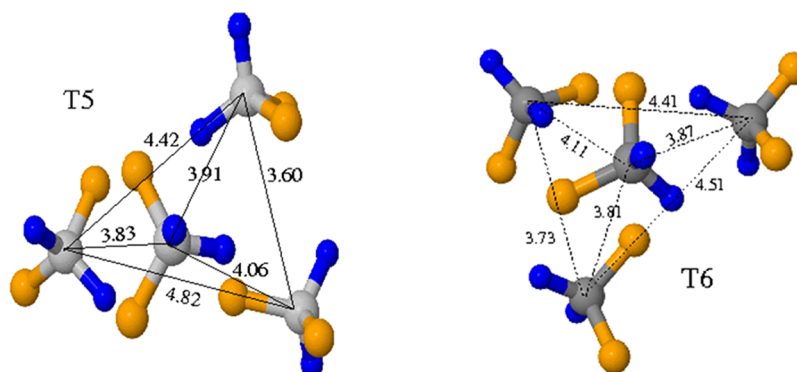


**Figure 6.** Geometrical structure of the two DFM tetramers having near tetrahedral conformation and marked with the T5 and T6 labels. Distances are between carbon atoms (Å).

the original paper and confirms the triangular structure of the most stable trimer. In Figure 4, it is apparent that all of the most stable trimers are of triangular form and differ from each other in the shape of the triangle having the C atoms as the vertex. The delicate interplay between attraction/repulsion between the F and H atoms yield at least four weak local minima, differing by less than 1 kcal/mol. The binding energy of the B1 and B2 structures is higher than that expected from a

linear arrangement, which may be roughly estimated as no more than two times the dimer energy,  $\sim 6$  kcal/mol. To gain a deeper insight into the WHB network that characterizes different trimers, the composite number  $N_{HF}$  may be introduced. Given an arrangement of two or more monomers,  $N_{HF}$  indicates the number of  $H\cdots F$  distances between different monomers in given ranges: the first digit is the number of  $H\cdots F$  distances in the 2.4–2.5 Å range, the second digit is the same in

Table 4. Comparison between Computed and Experimental Rotational Constants (MHz)<sup>a</sup>

oligomer	source	A	B	C	$\mu_A$	$\mu_B$	$\mu_C$	$\mu_{TOT}$
dimer	this work (A1)	6021.2	1259.8	1213.8	2.19	0.20	0.19	2.20
	exp <sup>6</sup>	6447.7	1290.2	1234.6				
trimer	this work (B1)	1322.5	804.6	592.8	2.14	0.63	0.44	2.28
	exp <sup>7</sup>	1336.4	820.5	592.7	strong	weak	weak	
tetramer	this work (T3)	835.9	403.6	313.1	2.85	0.12	0.47	2.89
	exp <sup>8</sup>	869.1	402.1	308.4				

<sup>a</sup>Dipole moments (Debye) along the principal inertia axes are also reported in the last columns.

Table 5. Shifts ( $\Delta\nu$ ) in CH Symmetric (s) and (a) Anti-symmetric Stretching Vibrational Frequencies and Average CH Equilibrium Bond Lengths Computed at the B97D Level for All Most Stable Oligomers<sup>a</sup>

oligomer	source	$\Delta\nu$ (cm <sup>-1</sup> )		$\Delta R_{CH}$ (mÅ)	
		s	a	H <sub>int</sub>	H <sub>ext</sub>
dimer	MP2/6-31G(d,p) <sup>6</sup>	+13	+20	-1.5 (3)	
dimer (A1)	this work	+24	+32	-2.3 (3)	-1.4 (1)
trimer (B1)	this work	+33	+49	-4.1 (4)	-1.7 (2)
tetramer (T3)	this work	+39	+54	-5.1 (4)	-1.2 (4)

<sup>a</sup>H<sub>int</sub> and H<sub>ext</sub> respectively, refer to H atoms involved or not involved in a H...F WHB. The total number of H<sub>int</sub> (H<sub>ext</sub>) atoms is reported in parentheses.

the 2.5–2.6 Å range, and so on, increasing the range by 0.1 Å. By looking at the last column of Table 2, it clearly appears that all triangular trimers are able to form 4 or 5 H...F bonds within 2.7 Å, whereas a linear disposition would allow for the formation of only two H...F and two H...F...H (or F...H...F) interactions, in which a single F (or H) atom shares two hydrogen bonds. This leads to a less efficient stabilization, which explains the higher stability of the triangular arrangements.

**Tetramer.** Starting from about 30 conformations extracted from the MC run, only 7 geometry optimizations lead to distinct geometries corresponding to local minima. Their rotational constants, dipole moments, and some other geometrical parameters are reported in Table 3. The structures are displayed in Figures 5 and 6, where some distances between the carbon atoms are shown.

Despite the fact that dispersion interactions may play an important role, it seems from Figures 5 and 6 that the most important force driving the stability of the tetramer is of electrostatic nature. In particular, the stability is increased by maximizing the number of H...F interactions between different molecules at distances in the range 2.4–2.7 Å. On the contrary, the F...F and H...H pairs are never found at similar distances but are always found at distances >2.8 and >3.1 Å, respectively. The interplay between attractive and repulsive forces gives rise to a large number of possible stable arrangements. In all cases, the distortion of the monomers from the DFM equilibrium geometry of the isolated molecule is very small. For instance, the H–C–F angles are 108.5° in the monomer and amount from 108.2° to 109.0° in the tetramers.

The most stable tetramer has a binding energy of 11.52 kcal/mol, corresponding to about 3.84 times the one of the most stable dimer. This indicates that tetramer binding energy is almost given by the sum of four pairs with geometries consistent with a rhomboidal geometry, as detailed in the following.

As expected, the reported structures are quasi degenerate, due to the large number of degrees of freedom of the system. Five local minima show a nearly planar conformation of the four carbon atoms (Figure 5), whereas conformers T5 and T6

assume a nearly tetrahedral-like conformation (Figure 6). The most stable conformation T1 shows an almost perfect square geometry for the C atoms, consistent with two very similar rotational constants, and belongs to the symmetry point group S<sub>4</sub>. T2 shows an almost perfect C<sub>i</sub> symmetry with the carbon atoms forming a rhombus. The null dipole moment of T1 and T2 is strictly connected with their symmetry properties since the totally symmetric representation of both S<sub>4</sub> and C<sub>i</sub> does not contain x nor y nor z. All of the other conformations do not show symmetry properties, and the dipole moment has no symmetry constraint.

Besides the T2 structure, conformations T3, T4, and T7 have a rhomboidal shape with different ratios between the major and minor diagonals, whose values are displayed in Figure 5. Conformers T3, T4, and T7 show also different deviations from planarity as concerns the four carbon atoms (see the LSP column in Table 3). In all cases, the major component of the dipole moment is along the major rotational constant, which corresponds to the minor inertia moment almost parallel to the major diagonal of the rhombus. Although some structures appear to be very similar to each other (for instance, T2 and T4), a careful analysis reveals that there are noticeable differences both in the dipole moment and in the number of short distance F...H pairs (see the last column of Table 3).

The tetramers identified by T5 and T6 labels have a different geometry with respect to all the other ones. As displayed in Figure 6, the carbon atoms assume a distorted tetrahedral form with the side length going from 3.60 to 4.51 Å, rather than a near planar conformation. The rotational constants are in the range as the previous ones, and the dipole moment takes again its maximum along the minor inertia moment.

Finally, a summary of the experimental and theoretical results for the three lowest oligomers of DFM are reported in Table 4. The very good agreement confirms that the integration between theory and experiment is able to provide useful information about this type of study.

## ■ BLUE SHIFTED HBS

To assess the presence of improper HBs, the symmetric and antisymmetric CH stretching frequencies were computed for the DFM monomer and for all of the most stable structures of the oligomers described in the above sections. The shift  $\Delta\nu$  for each oligomer was obtained by averaging the differences between the CH symmetric (antisymmetric) stretching frequencies of the molecular cluster and the monomer. Furthermore, the difference ( $\Delta R_{\text{CH}}$ ) between the CH bond lengths in the oligomers and that exhibited by the monomer was also examined. All data are summarized in Table 5.

The data computed for the dimer are in good agreement with those reported in ref 6, confirming the improper HB nature of the H...F interaction, as demonstrated by the blue shifts in both symmetric and antisymmetric stretching frequencies and by the shortening of the CH bond length. The connection between improper HBs and reduced CH distances is evident by looking at the different behavior of the internal H atoms ( $H_{\text{int}}$  forming HBs) and the external ones ( $H_{\text{ext}}$  not forming HB): the former show more marked contractions of the CH bond length. This observation indicates that the shortening of the CH bond lengths is due to the presence of fluorine atoms, and it is fully consistent with the unified explanation of the improper HB behavior given in ref 29. In this framework, the proper/improper behavior can find a rationale in terms of a delicate interplay of lengthening/contracting forces, where the former are connected with the attractive interaction between the positively polarized H and the electron rich F, whereas the latter are due to the electron affinity of the C atom.

The increasing trend in both vibrational blue shifts and  $\text{CH}_{\text{int}}$  bond shortening along the oligomer series can be rationalized by resorting again to the suggestions in ref 29, in terms of contracting and lengthening forces. The contracting force ascribed to the carbon electron affinity is of intramolecular nature, and it is expected to have a little dependence on the number of neighboring DFM monomer units. Conversely, the lengthening component remarkably depends on the strength of the HB involving the  $H_{\text{int}}$  atom, hence of intermolecular nature. Since the  $\text{CH}_{\text{int}}$  bond shortens by increasing the number of monomer units, the strength of the HB involving the  $H_{\text{int}}$  atom should also diminish along the series. As a matter of fact, the shortest intermolecular ( $\text{C}\cdots\text{C}$ ) distances are 3.52, 3.61, and 3.95 Å, for the dimer, trimer, and tetramer, respectively, indicating a gradual decrease of the HB strength along the series.

## ■ CONCLUSIONS

We have presented a theoretical study of the smaller oligomers of the DFM molecule. The method results from an integration of classical MC trajectories based on FF derived by quantum mechanical calculations and accurate DFT calculations at the state-of-the-art level. The structures of the tetramers identified as local minima show different geometries and properties, and it is singular that the most stable ones are not visible with MW spectroscopy, as they show high symmetry and null dipole moments. The agreement with experiment is excellent and seems to indicate that the search of local minima is rather complete.

## ■ AUTHOR INFORMATION

### Corresponding Author

\*E-mail: ivo.cacelli@unipi.it.

## Notes

The authors declare no competing financial interest.

## ■ REFERENCES

- (1) Banks, R. E.; Smart, B. E.; Tatlow, J. C. *Organofluorine Chemistry: Principles and Commercial Applications*; Plenum Press: New York, 1994.
- (2) Hiyama, T. *Organofluorine Compounds: Chemistry and Applications*; Springer: Berlin, 2000.
- (3) Soloshonok, V. A. *Enantiocontrolled Synthesis of Fluoro-Organic Compounds: Stereochemical Challenges and Biomedical Targets*; Wiley: New York, 2000.
- (4) Kirsh, P. *Modern Fluoroorganic Chemistry. Synthesis, Reactivity, Applications*; Wiley-VCH Verlag GmbH & Co. KGaA: Weinheim, Germany, 2004.
- (5) Kirsch, P.; Bremer, M. *Angew. Chem., Int. Ed.* **2000**, 39, 4216.
- (6) Caminati, W.; Melandri, S.; Moreschini, P.; Favero, P. G. *Angew. Chem., Int. Ed.* **1999**, 13, 2924.
- (7) Blanco, S.; Melandri, S.; Ottaviani, P.; Caminati, W. *J. Am. Chem. Soc.* **2007**, 129, 2700.
- (8) Feng, G.; Evangelisti, L.; Cacelli, I.; Carbonaro, L.; Prampolini, G.; Caminati, W. *Chem. Commun.* **2014**, 50, 171.
- (9) Cocinero, E. J.; Lesarri, A.; Ecija, P.; Basterretxea, F. J.; Grabow, J.-U.; Fernández, J. A.; Castano, F. *Angew. Chem., Int. Ed.* **2012**, 51, 3119.
- (10) Riley, K. E.; Pitoňák, M.; Cerny, J.; Hobza, P. *J. Chem. Theory Comput.* **2010**, 6, 66.
- (11) Thanthirawatte, K. S.; Hohenstein, E. G.; Burns, L. A.; Sherrill, C. A. *J. Chem. Theory Comput.* **2011**, 7, 88.
- (12) Zhao, Y.; Truhlar, D. G. *Theor. Chem. Acc.* **2007**, 120, 215.
- (13) Burns, L. A.; Vazquez-Mayagoitia, A.; Sumpter, B. G.; Sherrill, C. D. *J. Chem. Phys.* **2011**, 134, 084107.
- (14) Goerigk, L.; Grimme, S. *J. Chem. Theory Comput.* **2011**, 7, 291.
- (15) Grimme, S. *WIREs Comput. Mol. Sci.* **2011**, 1, 211.
- (16) Vazquez-Mayagoitia, A.; Sherrill, C. D.; Aprà, T.; Sumpter, B. G. *J. Chem. Theory Comput.* **2010**, 6, 727.
- (17) Vydrov, O. A.; Van Voorhis, T. *J. Chem. Phys.* **2010**, 133, 244103.
- (18) Grimme, S. *J. Comput. Chem.* **2006**, 27, 1787.
- (19) Grimme, S.; Antony, J.; Ehrlich, S.; Krieg, H. *J. Chem. Phys.* **2010**, 132, 154104.
- (20) Grimme, S. *J. Comput. Chem.* **2004**, 25, 1463.
- (21) Tsuzuki, S.; Honda, K.; Uchimaru, T.; Mikami, M.; Tanabe, K. *J. Am. Chem. Soc.* **2002**, 124, 104.
- (22) Hobza, P.; Zahradník, R.; Müller-Dethlefs, K. *Collect. Czech. Chem. Commun.* **2006**, 71, 443.
- (23) Sherrill, C. D.; Takatani, T.; Hohenstein, E. *J. Phys. Chem. A* **2009**, 113, 10146.
- (24) Rezáč, J.; Hobza, P. *J. Chem. Theory Comput.* **2013**, 9, 2151.
- (25) Hobza, P.; Spirko, V.; Selzle, H. L.; Schlag, E. W. *J. Phys. Chem. A* **1998**, 102, 2501.
- (26) Hobza, P.; Spirko, V.; Havlas, Z.; Buchold, K.; Reimann, B.; Barth, H. D.; Brutschy, B. *Chem. Phys. Lett.* **1999**, 299, 180.
- (27) Hobza, P.; Havlas, Z. *Chem. Rev.* **2000**, 100, 4253.
- (28) Cubero, E.; Orozco, M.; Hobza, P.; Luque, F. J. *J. Phys. Chem. A* **1999**, 103, 6394.
- (29) Joseph, J.; Jemmis, E. D. *J. Am. Chem. Soc.* **2007**, 129, 4620.
- (30) Li, A. Y.; Ji, H. B.; Cao, L. J. *J. Chem. Phys.* **2009**, 131, 164305.
- (31) Oliveria, B. G. *J. Chil. Chem. Soc.* **2011**, 56, 601.
- (32) Araújo, R. C. M. U.; Ramos, M. N. *J. Braz. Chem. Soc.* **1998**, 9, 499.
- (33) Dong-Fei, L.; Shu-Quin, G.; Cheng-Lin, S.; Zuo-Wei, L. *Chin. Phys. B* **2012**, 21, 083301.
- (34) Desiraju, G. R.; Steiner, T. *The Weak Hydrogen Bond in Structural Chemistry and Biology. IUCr Monographs on Crystallography*; Oxford University Press: Oxford, 2001; Vol. IX.
- (35) Steiner, T. *Angew. Chem., Int. Ed.* **2002**, 41, 48.
- (36) Delanoye, S. N.; Herrebout, W. A.; van der Veken, B. J. *J. Am. Chem. Soc.* **2002**, 124, 11854.

- (37) Cacelli, I.; Lami, C. F.; Prampolini, G. *J. Comput. Chem.* **2009**, *30*, 366.
- (38) Bizzarri, M.; Cacelli, I.; Prampolini, G.; Tani, A. *J. Phys. Chem. A* **2004**, *108*, 10336.
- (39) Halkier, A.; Helgaker, T.; Jorgensen, P.; Klopper, W.; Koch, H.; Olsen, J.; K. Wilson, A. K. *Chem. Phys. Lett.* **1998**, 286, 243.
- (40) Frisch, M. J.; et al. *Gaussian 09*, revision B.04; Gaussian Inc.: Pittsburgh, PA, 2008.
- (41) Boys, S. F.; Bernardi, F. *Mol. Phys.* **1970**, *19*, 553.